ORBITAL RESONANCES AND CHAOS IN THE SOLAR SYSTEM

Renu Malhotra

Lunar and Planetary Institute
3600 Bay Area Blvd, Houston, TX 77058, USA
E-mail: renu@lpi.jsc.nasa.gov

Abstract. Long term solar system dynamics is a tale of orbital resonance phenomena. Orbital resonances can be the source of both instability and long term stability. This lecture provides an overview, with simple models that elucidate our understanding of orbital resonance phenomena.

1. INTRODUCTION

The phenomenon of resonance is a familiar one to everybody from childhood. A very young child is delighted in a playground swing when an older companion drives the swing at its natural frequency and rapidly increases the swing amplitude; the older child accomplishes the same on her own without outside assistance by driving the swing at a frequency *twice* that of its natural frequency. Resonance phenomena in the Solar system are essentially similar – the driving of a dynamical system by a periodic force at a frequency which is a rational multiple of the natural frequency. In fact, there are many mathematical similarities with the playground analogy, including the fact of nonlinearity of the oscillations, which plays a fundamental role in the long term evolution of orbits in the planetary system. But there is also an important difference: in the playground, the child adjusts her driving frequency to remain in tune – hence in resonance – with the natural frequency which changes with the amplitude of the swing. Such self-tuning is sometimes realized in the Solar system; but it is more often and more generally the case that resonances come-and-go. And, as we shall see, resonances can be the source of both instability and long term stability.

There are three general types of resonance phenomena in the Solar system involving orbital motions: (i) *spin-orbit resonance*: this is a commensurability of the period of rotation of a satellite with the period of its orbital revolution; the "external driving" in this case is the gravitational tidal torque from the planet which is non-vanishing if the satellite is irregular in shape; (ii) *secular resonance*: this is a commensurability of the frequencies of precession of the orientation of orbits, as described by the direction of perihelion (or periapse) and the direction of the orbit normal; and (iii) *mean motion resonance*: this is intuitively the most obvious type of resonance in a planetary system; it occurs when the orbital periods of two bodies are close to a ratio of small integers. All of these are of course *self-excited* resonances, as they involve commensurabilities of the frequencies associated with internal degrees of freedom determined by gravitational forces internal

to the system. Fortunately, it is often possible to identify an unperturbed subsystem and separately a resonant perturbation, which facilitates the use of perturbation theory and other analytical and numerical tools.

This lecture provides an overview of these resonance phenomena in the Solar system, with simple models that elucidate our understanding. In a few instances, previously unpublished analysis or new derivation of known results is presented here for the first time. We have not attempted to provide a comprehensive guide to the literature, but we think that the bibliography should provide an adequate lead to it.

2. Spin-orbit resonances

Possibly the most familiar example of spin-orbit resonances is the spin-locked state of the Moon: only one hemisphere of the Moon is observable from the Earth because the Moon's rotation period around its own axis is equal to its orbital period around the Earth. Indeed, most natural satellites in the Solar system whose rotation rates have been measured are locked in this state, as are many known binary stellar systems. Another interesting Solar system example is the Pluto-Charon binary, where the spins of both the planet and the satellite are locked to their orbital motion, the final end-state of tidal evolution in binary systems.

The 1:1 spin-orbit resonance, also called the "synchronous" spin state, is mathematically a simple one, as its dynamics can be reduced to that of the common pendulum. Consider the idealized model of a non-spherically shaped satellite, with principal moments of inertia $A < B < C$, spinning about the axis of largest moment of inertia, and assume that the spin axis is normal to its orbital plane. The equation of motion for the spin is then given by

$$\ddot{\theta} = -\varepsilon \frac{GM}{r^3} \cos 2(\theta - f), \qquad \varepsilon \equiv \frac{3(B-A)}{2C} \tag{1}$$

where θ measures the orientation of the satellite's long axis relative to the direction of periapse of the orbit; G is the universal constant of gravitation, M is the planet's mass, $f = f(t)$ is the true anomaly (i.e. the longitude measured from the direction of periapse), and $r = r(t)$ is the distance from the planet. If the satellite has rotational symmetry, $B = C$, then there is no torque from the planet and the satellite's spin is unperturbed. If $B \neq C$, and the orbit is circular, then the equation is similar to that of the common pendulum:

$$\ddot{\theta} = -\varepsilon n^2 \sin 2(\theta - nt) \quad \text{or} \quad \ddot{\phi} = -2\varepsilon n^2 \sin \phi, \qquad \phi \equiv 2(\theta - nt), \tag{2}$$

where n is the orbital mean motion. This equation admits a librating solution in which the satellite's long axis librates about the planet-satellite direction and its mean spin rate equals its orbital mean motion. This is the oft-observed synchronous spin state. The pendulum analogy shows directly that the width of the 1:1 spin-orbit resonance is

$$\Delta \dot{\theta} = 2\sqrt{2\varepsilon} n. \tag{3}$$

38
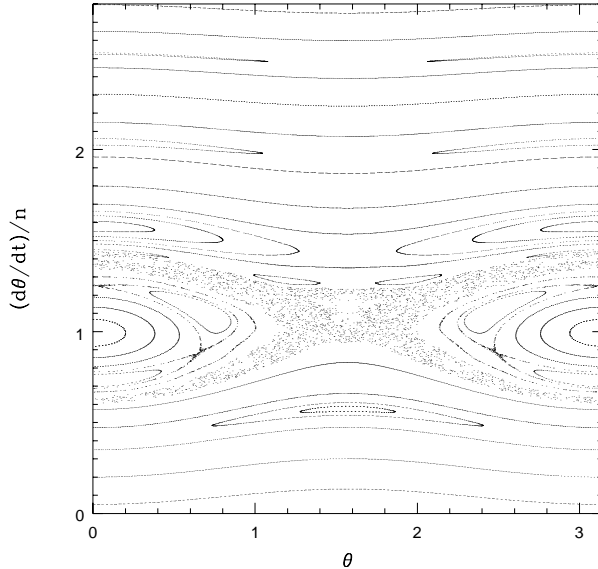
Figure 1.   Surface-of-section generated by the spin-orbit model of Eqn. 1, for
$\varepsilon = 0.075$ and orbital eccentricity, $e = 0.02$.

However, other spin-orbit resonances are also possible. Consider the case when the orbit is non-circular. For small eccentricity, we can expand the right hand side of Eqn. 1 in a power series in e:

$$\ddot{\theta} = -\varepsilon n^2 \Big[\sin 2(\theta - nt) - \frac{1}{2}e\Big(\sin(2\theta - nt) - 7\sin(2\theta - 3nt)\Big) + \mathcal{O}(e^2)\Big]. \qquad (4)$$

At the first order in eccentricity, there are two new terms corresponding to the 1:2 and the 3:2 spin-orbit resonances. The planet Mercury is the best known Solar system example of the 3:2 spin-orbit resonance, with its orbital period of 88 days and rotation period of 59 days. The width of the 3:2 spin-orbit resonance is a factor $\sqrt{7e/2}$ smaller than the 1:1. For Mercury, whose orbital eccentricity is 0.2, this factor is ~ 0.84, so that the 3:2 resonance is nearly as strong as the 1:1. However, most satellites which are close to their planets have very small orbital eccentricities, typically < 0.01, so that the 3:2 spin-orbit resonance width is considerably smaller than that of the 1:1. Other spin-orbit resonances are even narrower. Fig. 1 shows the structure of the spin-orbit phase space determined by the simplified model of Eqn. 1, for values of parameters ε and e which are slightly exaggerated from typical values for satellites in the Solar system. Note the qualitative features of this phase space structure: resonance widths small compared to the resonance spacings, and mostly regular, quasiperiodic phase space trajectories.

If we consider that the primordial spin period of solid bodies in the Solar system is in-ferred to be on the order of hours and orbital periods of satellites are on the order of days, and that the width in frequency space of spin-orbit resonances is relatively very small (given the usually small deviations from spherical shapes and the usually small orbital eccentricities of planetary bodies) a reasonable conclusion is that the observed ubiquity

39

of spin-orbit resonances is not simply due to randomly favorable initial conditions, but rather a consequence of a common physical effect.

Tidal torques from the planet and internal friction in the satellite have widely been understood to be the cause of spin-orbit coupling. These torques cause a slowing down of the satellite's primordial spin rate. As it de-spins, a satellite may encounter several spin-orbit resonances. The "separatrix" or boundary of each spin-orbit resonance is a chaotic zone, owing to the perturbations from other neighboring spin-orbit resonances (cf. Fig. 1). In these boundary regions the spin rate is erratic. Entering a spin-orbit resonant state requires the crossing of a chaotic separatrix; this is a deterministic but chaotic process, and has probably occurred many times in the history of most Solar system satellites (as well as Mercury, and possibly Pluto and Charon), before the final stable spin state is achieved.

There is one well known exceptional case in the Solar system where the spin-orbit phase space is qualitatively different from that of Fig. 1. The satellite Hyperion of Saturn has a highly irregular shape and a large orbital eccentricity of 0.104. (The latter possibly owes to forcing by a mean motion resonance with another satellite, Titan, but this conclusion is uncertain.) Consequently, the widths of the spin-orbit resonances are so large that neighboring resonances overlap greatly, and their chaotic separatrices merge to create a large "chaotic sea" in the spin-orbit phase space of this satellite. The libration zone of the synchronous spin state "dissolves" in a chaotic sea, and the satellite is unable to maintain stable synchronous spin. Indeed, it has been shown that for this satellite, not only is the spin rate erratic, but the orientation of its spin axis also changes chaotically (Wisdom *et al.*, 1984; Klavetter, 1989; Black *et al.*, 1995).

3.   Orbit-orbit Resonances: an introduction

Consider the simplest planetary system consisting of only one planet around the Sun. In this system, there are three degrees of freedom, corresponding to the three spatial degrees of freedom for the planet[1]. The three degrees of freedom can be described by three angular variables, one of which measures the motion of the planet in its elliptical orbit and the other two describe the orientation of the orbit in space (Fig. 2). In the idealized system of two point masses, the orbit orientation is fixed in space, and there is only one non-vanishing frequency, namely, the frequency of revolution around the Sun. But in the realistic system, there are other perturbations, such as the gravitational forces from other planets (and, as in the case of satellite systems, the perturbations from the non-spherical shape of the primary), which cause changes in the shape and orientation of the elliptical orbit. Thus, what at first glance would appear to be only a one-frequency

---

[1]The additional three degrees of freedom for the Sun can be made ignorable by using the coordinates of the planet relative to the Sun and using the "reduced mass", $m_{\mathrm{sun}}m_{\mathrm{planet}}/(m_{\mathrm{sun}} + m_{\mathrm{planet}})$, thus reducing the problem to an equivalent *one body problem*. For multiple planets around the Sun, we can again remove the degrees of freedom corresponding to the Sun by using a special coordinate system invented by Jacobi in which we use the coordinates of the first planet relative to the Sun, then the coordinates of the second planet relative to the center-of-mass of the Sun and first planet, and so on for any number of planets.
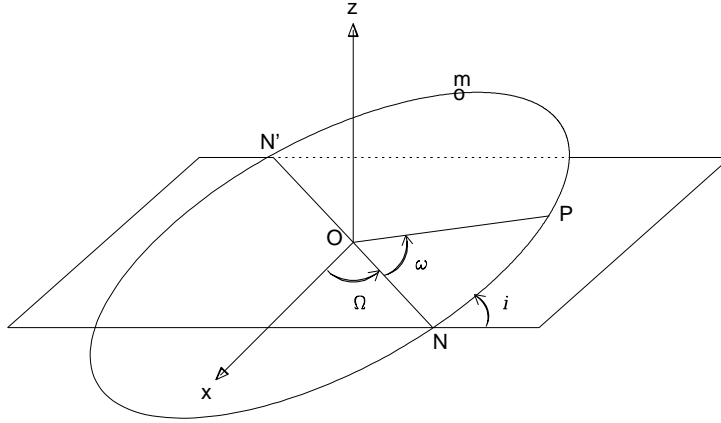
Figure 2.   Elements of the Keplerian orbit: a particle, m, traces out an ellipse of *semimajor axis a* and *eccentricity e*, with the Sun at one focus of the ellipse (which is the origin of the heliocentric coordinate system indicated here). The plane of the orbit has *inclination i* with respect to the fixed reference plane, and intersects the latter along the line of nodes, NN', where ON defines the *ascending node*. The long axis of the ellipse is along PP', where OP defines the perihelion (or periapse); the *argument of perihelion ω* is measured with respect to ON in the orbital plane. The *mean anomaly* is the mean angular motion of the particle measured from OP.

system is actually one with three frequencies: the first frequency is the obvious one of revolution around the Sun, and the other two are the slow frequencies of precession of the direction of perihelion and the pole of the orbit plane.

In a multi-planet system, secular resonances involve commensurabilities amongst the latter slow frequencies of orbital precession, while mean motion resonances are commensurabilities of the frequencies of orbital revolution. In most cases in the Solar system, there is a clear separation of the secular precession and orbital mean motion timescales, but there is also a coupling between the two which leads to chaotic dynamics. The boundaries (or separatrices) of mean resonances are often the site for such interactions between secular and mean motion resonances. There also exists in the Solar system one example of a 'hybrid' resonance involving a commensurability of a secular precession frequency with an orbital mean motion: the angular velocity of the apsidal precession rate of a ringlet within the C-ring of Saturn is commensurate with the orbital mean motion of Titan. This has come to be called the Titan 1:0 apsidal resonance.

4. Secular resonances

4.1. A toy model

The phenomenon of secular resonance is most simply illustrated with a toy model of the planar elliptic restricted three body problem in which the orbit of the primaries, e.g. Sun and one planet, is assumed to be a *precessing* ellipse of fixed semimajor axis, a_{p}, eccentricity, e_{p}, and precession rate $\dot{\varpi}_{\mathrm{p}} = g_{\mathrm{p}}$. The unperturbed orbit of a test particle in this model is simply the usual keplerian ellipse in the central $1/r$ potential. However, the average gravitational force of the planet perturbs the shape and orientation of the orbit. This perturbation can be described as a slow precession of the elliptical orbit. The precession rate, g_0, is proportional to the mass of the perturbing planet and is also a function of the orbital semimajor axis of the particle relative to that of the planet. A secular resonance occurs when the induced precession rate, g_0, equals that of the planet's own orbital precession rate, g_{p}. The effect of such a resonance is to amplify the orbital eccentricity of the particle, as we see below.

The secular perturbations of the test particle's orbit are described by the following Hamiltonian function:

$$H_{\mathrm{sec}} = -\frac{m_{\mathrm{p}}}{a_m}\Big\{A_0(\alpha) + A(\alpha)e^2 + B(\alpha)e^4 - C(\alpha)ee_{\mathrm{p}}\cos(\varpi_{\mathrm{p}} - \varpi)\Big\}. \tag{5}$$

This function represents the first few terms in a series expansion in powers of the orbital eccentricities of the orbit-averaged disturbing potential of the planet on the test particle. Units are chosen so that the universal constant of Gravitation, G, the sum of the masses of the primaries, $M_{\odot} + m_{\mathrm{p}}$, and their orbital semimajor axis, a_{p}, are all unity. The symbols are as follows: $a_m = \max(a, a_{\mathrm{p}})$ and $\alpha = \min\{a/a_{\mathrm{p}}, a_{\mathrm{p}}/a\}$ where a is the semimajor axis of the test particle, ϖ and ϖ_{p} are the longitude of periapse of the test particle and of the planet's orbit, respectively; and the coefficients A_0, A, B, C are functions of α expressed in terms of Laplace coefficients:

$$
\begin{aligned}
A(\alpha) &= \frac{1}{8}\alpha b_{3/2}^{(1)}(\alpha), \\
B(\alpha) &= \frac{1}{128}\alpha^3 \frac{d^2}{d\alpha^2}b_{3/2}^{(1)}(\alpha) && \text{for } a < a_{\mathrm{p}}, \\
&= \frac{1}{128}\alpha^2\Big(12 + 8\alpha\frac{d}{d\alpha} + \frac{d^2}{d\alpha^2}\Big)b_{3/2}^{(1)}(\alpha) && \text{for } a > a_{\mathrm{p}}, \\
C(\alpha) &= \frac{1}{4}\alpha b_{3/2}^{(2)}(\alpha).
\end{aligned}
\tag{6}
$$

To obtain the dynamical equations for the secular perturbations in the most straightforward manner using Hamilton's equations, we can use the canonically conjugate Delaunay variables, $-\varpi$ and $J = \sqrt{a}(1 - \sqrt{1 - e^2})$. In terms of these, we can write

$$H_{\mathrm{sec}} = -\frac{m_{\mathrm{p}}}{a_m}A_0(\alpha) - g_0 J + \beta J^2 + \varepsilon\sqrt{2J}\cos(\varpi - \varpi_{\mathrm{p}}), \tag{7}$$

where

$$g_0 = \frac{2A(\alpha)}{a^{\frac{1}{2}}a_m}m_{\mathrm{p}}, \qquad \beta = \frac{A(\alpha) - 4B(\alpha)}{aa_m}m_{\mathrm{p}}, \qquad \varepsilon = \frac{C(\alpha)}{a^{\frac{1}{4}}a_m}m_{\mathrm{p}}e_{\mathrm{p}}. \tag{8}$$

The first term alters slightly the orbital mean motion but does not affect the orbital shape or orientation. The remaining three terms describe the dynamics of a nonlinear oscillator. The coefficient β of the nonlinear term is quite small when α is not too close to 1. Consequently, if we neglect the nonlinear term, the dynamics of the secular resonance is similar to the usual resonantly forced harmonic oscillator, as we can see by writing Hamilton's equations for the Poincaré variables, $(x, y) = \sqrt{2J}(\cos\varpi, -\sin\varpi)$:

$$\dot{x} = g_0 y + \varepsilon \sin(g_{\mathrm{p}}t + \varpi_{p,0}), \qquad \dot{y} = -g_0 x + \varepsilon \cos(g_{\mathrm{p}}t + \varpi_{p,0}), \tag{9}$$

where we have used $\varpi_{\mathrm{p}} = g_{\mathrm{p}}t + \varpi_{p0}$. These equations have the following solution for forced oscillations:

$$\left\{x(t), y(t)\right\}_{\mathrm{forced}} = \frac{\varepsilon}{g_0 - g_{\mathrm{p}}}\left\{\cos(g_{\mathrm{p}}t + \varpi_{p,0}), -\sin(g_{\mathrm{p}}t + \varpi_{p,0})\right\}. \tag{10}$$

Furthermore, at exact resonance, i.e. $g_0 = g_{\mathrm{p}}$, we have the particular solution of the resonantly forced oscillations whose amplitude grows without bound:

$$\left\{x(t), y(t)\right\}_{\mathrm{resonance}} = \varepsilon t \left\{\sin(g_{\mathrm{p}}t + \varpi_{p,0}), \cos(g_{\mathrm{p}}t + \varpi_{p,0})\right\}. \tag{11}$$

However, when $g_0 \approx g_{\mathrm{p}}$, the non-linear terms limit the growth of the eccentricity. An estimate of the maximum amplitude can be obtained by a rigorous analysis of Eqn. 7 (see Section 5.3 below for details). For orbits with initial $(x, y) = (0, 0)$, the maximum excitation occurs at $g_0 = g_{\mathrm{p}} + 3(\beta\varepsilon^2/2)^{1/3}$, and the maximum amplitude is given by

$$J_{\mathrm{max}} = 2\left|\frac{2\varepsilon}{\beta}\right|^{\frac{2}{3}} \qquad \text{or} \qquad e_{\mathrm{max}} \approx 2\left|\frac{2C}{A - 4B}e_{\mathrm{p}}\right|^{\frac{1}{3}}. \tag{12}$$

Note that the timescale for the growth of the amplitude is inversely proportional to the mass and eccentricity of the perturber, but e_{max} is independent of the perturber mass, μ, and proportional to a low, one-third power of its eccentricity. Furthermore, the coefficient $|A - 4B|$ is quite small over a large range of test particle semimajor axis, such that initially circular orbits close to a secular resonance can be forced to very high eccentricities, even for quite modest values of the planet's eccentricity.

4.2. Examples of minor planets at secular resonances

It is well known that the inner edge of the asteroid belt is close to the so-called ν_6 secular resonance defined by $g_0 \approx g_6$, where $g_6 \simeq 28.25''/\mathrm{yr}$ is one of the fundamental modes of the planetary system and approximately the mean perihelion precession rate of Saturn's orbit. We can derive a secular Hamiltonian for the ν_6 resonance experienced by an asteroid by summing the secular terms of the form given in Eqn. 5 in the perturbation potential due to each of the Jovian planets, and representing the secular motions of the planets themselves as a superposition of the fundamental modes, keeping only the ν_6 resonant terms. Then,

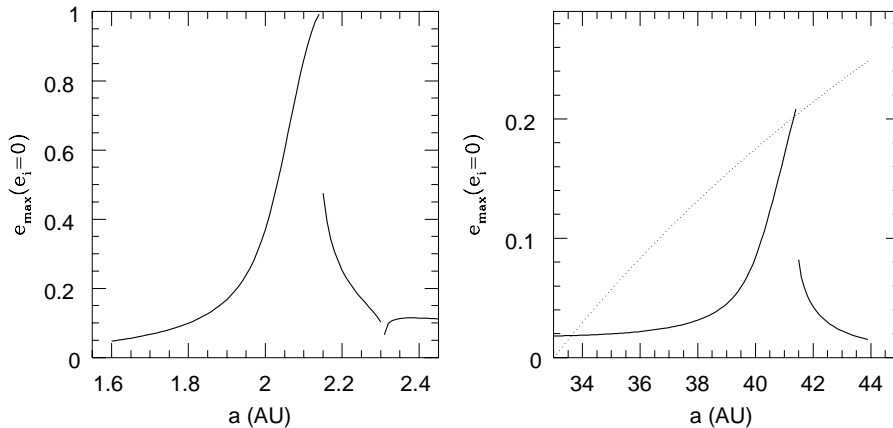$$H_{\mathrm{sec}} = -g_0 J + \beta J^2 + \varepsilon\sqrt{2J}\cos(\varpi_6 - \varpi), \tag{13}$$

43

Figure 3. Maximum eccentricity excited on initially circular orbits by the ν_6 resonance in the asteroid belt (left), and the ν_8 resonance in the Kuiper Belt (right). The dotted line on the right indicates orbits perihelion at 33 AU.

with

$$g_0 = \sum_i \frac{2A(\alpha_i)}{a^{\frac{1}{2}}a_i}m_i, \qquad \beta = \sum_i \frac{A(\alpha_i) - 4B(\alpha_i)}{aa_i}m_i, \qquad \varepsilon = \sum_i \frac{C(\alpha_i)}{a^{\frac{1}{4}}a_i}m_iE_i^{(6)}. \qquad (14)$$

where the summations are over the Jovian planets, $E_i^{(6)}$ is the amplitude of the g_6 mode in the orbit of the i-th planet, $\alpha_i = a/a_i$ is the ratio of the asteroid and i-th planet's semimajor axes, and A, B, C are the same functions defined in Eqn. 6 above.

For initially circular asteroid orbits, the results of the above simple analytical model for the eccentricity excitation by the ν_6 resonance is shown in Fig. 3a as a function of asteroid semimajor axis. We see that at the inner edge of the asteroid belt, near 2 AU, the ν_6 secular resonance excites eccentricities in excess of 0.3. Such orbits would be Mars and Earth-crossing. Of course, the low order and the severe simplifications of this analysis are suspect for such large eccentricities, but the qualitative conclusion on the dramatic instability induced by this secular resonance is robust. A more complete analysis, including inclined asteroid orbits, shows that the location of the ν_6 secular resonance defines the inner boundary of the main asteroid belt (Knezevic *et al.*, 1991; Morbidelli 1993). It is suspected that this resonance provides a transport route to the terrestrial planets and even directly to the Sun for asteroids injected into it by means of random collisions or other perturbations elsewhere in the main asteroid belt (Farinella *et al.*, 1994; Morbidelli *et al.*, 1994).

A similar application is in the trans-Neptunian region. Applying the above resonance model, with parameters appropriate to the g_8 mode (approximately the mean precession rate of Neptune's orbit), the eccentricity excitation due to the ν_8 resonance in the trans-Neptunian region is shown in Fig. 3b. This figure shows that near-circular orbits with $a \approx 41$ AU achieve perihelion distances less than 33 AU where Neptune's non-secular perturbations are strong. Numerical simulations show that such orbits are highly chaotic

44

and are dynamically short-lived (Levison and Duncan, 1993; Holman and Wisdom, 1993). Observationally, this location coincides with an apparent gap in the distribution of the recently discovered trans-Neptunian Kuiper Belt population of minor planets (Jewitt *et al.*, 1996).

Secular resonances also occur embedded within or in close proximity to mean motion resonances in the asteroid belt as well as in the Kuiper Belt, with interesting phenomenological implications (Morbidelli and Moons, 1993; Morbidelli, 1997; Malhotra, 1998).

One specific secular resonance, called the "Kozai resonance" or the "Kozai mechanism" after Y. Kozai (1962), is defined by the 1:1 commensurability of the secular precession rates of the perihelion and the orbit normal such that the argument of perihelion is stationary (or librates). This resonance, which generally requires significant orbital eccentricity and inclination, causes coupled oscillations of these two orbital elements (with little or no perturbation of the semimajor axis). It is likely a common, if intermittent, feature in the long term dynamics of many minor planets. A particularly well known example is Pluto whose argument of perihelion librates about 90 degrees (Malhotra and Williams, 1997). The Kozai mechanism has been invoked to explain the high eccentricity orbit of a recently discovered extra-solar planet (Holman *et al.*, 1997).

4.3. Secular resonances amongst the major planets

Self-excited secular resonances amongst the major planets determine the long term dynamical stability of the planetary system. This is a topic of current research with many poorly understood aspects; only some introductory remarks will be made here. In the linear approximation, the perturbations of the major planets (neglecting Pluto[2]) due to their mutual gravitational forces are described by a set of coupled linear differential equations for the so-called eccentricity and inclination vectors defined by $\{h_j, k_j\} = e_j\{\sin\varpi_j, \cos\varpi_j\}$, and $\{p_j, q_j\} = \sin i_j\{\sin\Omega_j, \cos\Omega_j\}$:

$$
\begin{aligned}
\frac{d}{dt}\{h_j, k_j\} &= \sum_{l=1,8} M_{jl}\{k_l, -h_l\}, \\
\frac{d}{dt}\{p_j, q_j\} &= \sum_{l=1,8} N_{jl}\{q_l, -p_l\},
\end{aligned}
\tag{15}
$$

where the coefficients, M_{jl} and N_{jl}, which are proportional to the planetary masses and depend upon the orbital semimajor axes, can be considered to be constant in the first approximation. The general solution is a linear combination of eigenmodes:

$$
\begin{aligned}
\{h_j, k_j\} &= \sum_{l=1,8} E_j^{(l)}\{\cos(g_l t + \beta_l),\ \sin(g_l t + \beta_l)\}, \\
\{p_j, q_j\} &= \sum_{l=1,8} I_j^{(l)}\{\cos(s_l t + \gamma_l),\ \sin(s_l t + \gamma_l)\}.
\end{aligned}
\tag{16}
$$

---

[2]Pluto's mass is a fraction of a percent of the Earth's mass, and its average distance from the other planets is large, so neglecting its secular perturbations on the other major planets is a reasonable approximation.

We note that, at the linear order, the h, k and p, q are decoupled from each other, and their time variation is quasiperiodic. The fundamental frequencies g_l, s_l in the spectrum of h, k, p, q have periods ranging from 46,000 yr to 1.9 million yr (Brouwer and Clemence, 1961), approximately four orders of magnitude longer than the orbital periods.

During the early part of the 20th century, considerable effort was expended on refining the calculations for planetary motions, motivated in large part by the need for accurate timekeeping for navigation. High order (analytic) perturbation series were developed, which included corrections to the linear secular theory arising from nonlinear couplings amongst the (h, k, p, q) variables as well as from the effects of near-resonances amongst the orbital mean motions of the planets. An orderly perturbation theoretic approach shows that nonlinear secular terms cause small shifts in the fundamental frequencies and also lead to frequency modes which are linear combinations of the fundamental modes. Although this approach has been used for decades (and is justifiable for the practical purpose of calculating planetary motions on "human" timescales), there is no mathematical proof of the validity of the results for long periods of time. In fact, the nonlinear couplings amongst the secular variables (h, k, p, q) allow for self-excited secular resonances with frequencies close to zero, and formal perturbation series fail to converge.

It is inevitable that at some level, we approach a non-perturbative regime where there is an insufficient separation of neighboring resonances and a quasi-periodic solution becomes untenable. The universal consequence of overlapping nonlinear resonances is chaos, similar to the overlapping resonances discussed above in the context of spin-orbit coupling. Qualitatively, the long term orbital evolution is such that the nearly quasi-periodic solution is interrupted intermittently by chaotic variations arising from a drift across secular resonances and associated chaotic layers; the most dramatic changes occur in the angular orbital elements, resulting in a rapid loss of phase information; a less dramatic but significant chaotic diffusion is induced in the orbital eccentricities and inclinations. There is numerical evidence that such chaotic secular resonance crossings occur at the lowest possible order in the long term dynamics of the terrestrial planets (Laskar, 1994). A particular consequence is that Mercury's orbital eccentricity varies chaotically on timescales of only tens of millions of years, with large-scale excursions of its eccentricity possible on 10^9-year timescales. The reader is referred to (Laskar, 1996) for further commentary on the implications of this result.

5. Mean motion resonances

5.1. Introduction

There are many examples of commensurabilities of the mean orbital angular velocities of Solar system bodies; the most striking ones are indicated in Fig. 4. We note that the definition of *exact* commensurability requires a rather high precision of tuning of the orbital frequencies which would allow a resonance angle libration such that the time-averaged rate of change of the resonance angle vanishes:

$$\begin{aligned} \Delta n/n \;\; &\sim \;\; \mu^{\frac{2}{3}} \;\;\; \text{or} \;\;\; (\mu e)^{\frac{1}{2}} \;\;\; \text{for a first order resonance,} \\ \Delta n/n \;\; &\sim \;\; \mu \;\;\; \text{or} \;\;\; (\mu e^2)^{\frac{1}{2}} \;\;\; \text{for a second order resonance,} \end{aligned} \tag{17}$$
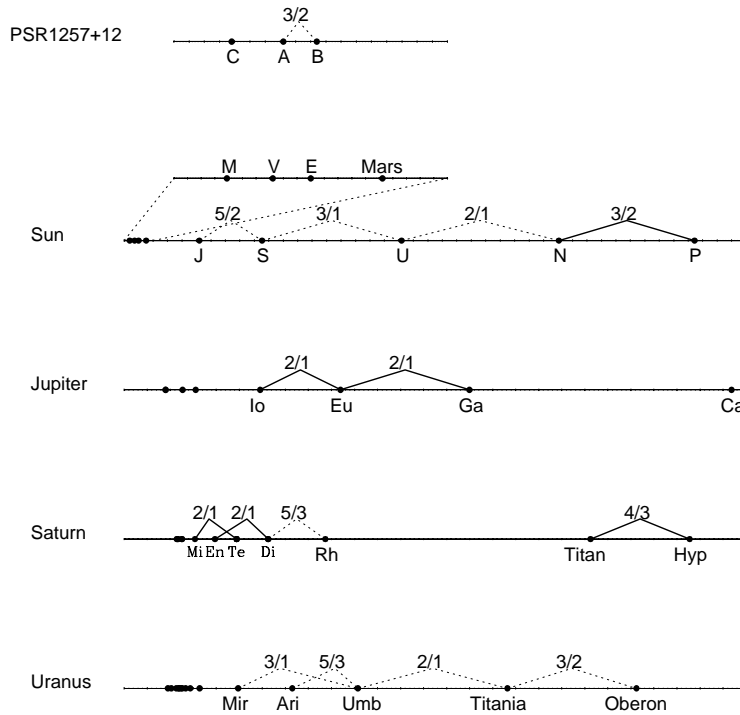
Figure 4. The relative orbital spacings of major planets and satellites of the Solar system. Exact mean motion resonances are indicated by solid lines; near-resonances are indicated by dotted lines. The planetary system of the millisecond pulsar, PSR1257+12 is also shown.

where μ is the ratio of planet mass to that of the Sun, the first quantity on the rhs applies to near-circular orbits while the second estimate is for orbits of significant eccentricity. Amongst the major planets, only one pair, Neptune and Pluto, actually satisfies a resonance angle libration condition; the well-known 5:2 near-resonance between Jupiter and Saturn is just that – only a near-resonance, as are the 2:1 between Uranus and Neptune and the 3:1 between Saturn and Uranus. Several efforts have been made to identify a precise resonant structure of the planetary system, but the departures from exact resonance are sufficiently large that no significance has been identified for the near-commensurabilities. The resonance libration of Neptune and Pluto is therefore particularly intriguing. Plausible explanations for this resonance have been formulated only in the last few years, and suggest an origin in the dynamical processes of planet formation (Malhotra, 1993; Malhotra, 1995; Malhotra and Williams, 1997). Also shown in Fig. 4 is the only confirmed extra-solar planetary system, the planets around the millisecond pulsar PSR1257+12, which also exhibits a near-resonant, *but not exact resonant*, orbital configuration.

Somewhat in contrast with the planetary system, the satellite systems of the giant planets Jupiter and Saturn (but not Uranus) exhibit many exact mean motion resonances, as indicated in Fig. 4. Following a suggestion by T. Gold (quoted in Goldreich, 1965), the origin of these exact resonances has been generally understood to be the consequence of very small tidal dissipation effects which alter the orbital semimajor axes sufficiently over billion year timescales that initially well separated non-resonant orbits (or perhaps near-resonant orbits) evolve into an exact resonance state. Once a resonance libration is established, it is generally stable to further adiabatic changes in the individual orbits due to continuing dissipative effects. This idea has been examined in some detail and the evidence appears to be in its favor in the most prominent cases of mean motion commensurabilities amongst the Jovian and Saturnian satellites. (See Peale (1986) for a review.) However, the Uranian satellites presented a challenge to this view, as there are no exact resonances in this satellite system, and it is unsatisfactory to argue that somehow tidal dissipation is vastly different in this system. An interesting resolution to this puzzle was achieved when the dynamics of orbital resonances was analyzed carefully and the role of the small but significant splitting of mean motion resonances and the interaction of neighboring resonances was recognized. Such interactions can destabilize a previously established resonance, so that mean motion resonance lifetimes can be much shorter than the age of the Solar system. More recent numerical analysis and modeling of the Jovian satellites, Io, Europa and Ganymede, also suggest a dynamic, evolving orbital configuration on billion year timescales (Showman and Malhotra, 1997). We discuss the evolution into and out of mean motion resonances in some detail below.

Not indicated in Fig. 4 is the distribution of small bodies in the Solar system. The most prominent and well known populations are in the asteroid belt between Mars and Jupiter and in the Kuiper Belt beyond Neptune; others include a large population of Trojan asteroids at the Lagrange points of Jupiter, a population of near-Earth asteroids, a class of objects called Centaurs found on chaotic planet-crossing orbits between Jupiter and Neptune, and the comets with several distinct subgroups amongst them. Resonance dynamics plays a critical role in understanding the distribution and transport of these small bodies, as well as interplanetary dust particles, in various regions of the planetary system. Also omitted from Fig. 4 are the varied and extensive ring systems of the outer planets which are sometimes described as analogs for protoplanetary disks and laboratories for resonance theories. They exhibit many dynamical features associated with orbital resonance phenomena (Goldreich & Tremaine, 1982).

5.2. Mean motion resonance splitting

The discussion below provides an introduction to useful analytical models and tools that aid in the understanding of the dynamics of orbital mean motion resonances. One of the most fundamental points to appreciate about mean motion resonances is the fact of their multiplicity. This is revealed in a power series expansion of the mutual perturbation potential of a pair of satellites orbiting a primary in orbits that are close to resonance; for the $p : p + q$ resonance, the series contains terms in the form

$$V_{p,q} = -\frac{m_1 m_2}{a_2}\Big\{ \sum_{r=0}^{q} C_{pr}\, e_1^r\, e_2^{q-r} \cos[(p+q)\lambda_2 - p\lambda_1 - r\varpi_1 - (q-r)\varpi_2]$$
$$+ \sum_{r=0}^{q} D_{pr}\, i_1^r\, i_2^{q-r} \cos[(p+q)\lambda_2 - p\lambda_1 - r\Omega_1 - (q-r)\Omega_2] \Big\}. \qquad (18)$$

As before, we assume that units are chosen so that the universal constant of gravitation, G, and the mass of the primary, M, are unity. The subscripts 1 and 2 refer to the inner and outer satellites, respectively; p and $q > 0$ are integers, λ's are the instantaneous mean longitudes of the satellites, and ϖ and Ω are the longitudes of periapse and ascending node. For every pair, p, q, there are $q + 1$ lowest order terms in the eccentricity, and also $q+1$ terms in the inclination. The eccentricity-type resonances appear at the first order in eccentricity, but the inclination terms appear only for even values of q, thus no less than the second order in inclination. This is simply a consequence of the physical constraint of rotational invariance of the potential. (The eccentricity-type and the inclination-type resonances are coupled through higher-order near-resonant terms as well secular terms not listed in Eqn. 18. The interested reader is referred to (Hamilton, 1994; Ellis & Murray, 1998) for recent accessible discussions of the properties of the perturbation potential.)

The nominal location of the $p : p + q$ mean motion resonance is defined by $(p + q)n_2 - pn_1 \approx 0$, but the resonance is actually split into several subresonances defined by each distinct term in the series in Eqn. 18. The locations of the subresonances differ by $\sim (\dot\varpi_1 - \dot\varpi_2)$ and $\sim (\dot\Omega_1 - \dot\Omega_2)$ in frequency, or $\Delta a_j/a_j \sim (\dot\varpi_1 - \dot\varpi_2)/n_1$ in semimajor axis, where $\dot\varpi_j, \dot\Omega_j$ are the (usually small) secular rates of precession of the periapses and nodes.

If the splitting between neighboring subresonances is much greater than the sum of their half-widths, each subresonance can be analyzed in isolation. The single resonance description is also appropriate in the other limit, when the splitting is exceedingly small compared to the widths and all the subresonances collapse into a single resonance. In both these limiting cases, only a very thin chaotic layer is present at the resonance separatrix. On the other hand, when the separation between neighboring resonances is comparable to their widths, the interaction between resonances is strong and a strong instability of the motion occurs: most orbits in the vicinity of the resonances are chaotic, with stable resonance-locking possible only in very narrowly restricted regions of the phase space. All of these regimes of resonance overlap – from strong to weak – are realized in the Solar system.

5.3. A simple analytical model for an isolated resonance

For specificity, let us consider an isolated first order interior eccentricity-type $p : p + 1$ resonance, neglecting the perturbations on the outer satellite. (The analysis here is easily adapted for exterior resonances, with only a few modifications in the definitions of coefficients; it is also readily extended to higher order resonances.) The essential lowest order perturbation terms seen by the inner body near resonance are given by

$$V/m_1 = -\mu\Big\{ A(\alpha)e^2 + B(\alpha)e^4 - C(\alpha)e \cos[(p+1)n_2 t - p\lambda - \varpi] \Big\}, \qquad (19)$$

49

where $\alpha = a_1/a_2, \mu = m_2/M$, and we have chosen a unit of length equal to a_2, and we have dropped the subscript 1 on the orbital elements of m_1. With little error, we may evaluate the coefficients $A(\alpha), B(\alpha), C(\alpha)$ at $\alpha = \alpha_{\mathrm{res}} = (1 + 1/p)^{-2/3}$. The expressions for $A(\alpha)$ and $B(\alpha)$ are as before (Eqns. 6), and the coefficient $C(\alpha)$ of the resonant term is given by

$$C(\alpha) = \frac{1}{2}\Big[2(p+1) + \alpha\frac{d}{d\alpha}\Big]b_{1/2}^{(p+1)}(\alpha). \tag{20}$$

Although m_1 has two degrees of freedom, we can simplify the analysis by identifying the fast and slow degrees of freedom and analyzing the dynamics of the slow (resonance) variables. This is done most readily by use of a linear combination of the canonical Delaunay variables:

$$\phi = (p+1)n_2 t - p\lambda - \varpi, \qquad J = \sqrt{a}(1 - \sqrt{1 - e^2}) \simeq \frac{1}{2}\sqrt{a}e^2(1 + \frac{1}{4}e^4),$$
$$\lambda, \qquad\qquad\qquad K = \sqrt{a}[1 + p(1 - \sqrt{1 - e^2})]. \tag{21}$$

The pair (ϕ, J) are the canonically conjugate resonance variables and represent the slow degree of freedom. The Hamiltonian function for m_1 is

$$H = -1/2a + (p+1)n_2 J + V/m_1, \tag{22}$$

which can be expanded in a power series in J to obtain the following single resonance Hamiltonian[3]:

$$H = \omega J + \beta J^2 + \varepsilon\sqrt{2J}\cos\phi, \tag{23}$$

where

$$\omega = (p+1)n_2 - pn^\star - g_0, \qquad n^\star = K^{-3}, \quad g_0 = \frac{2A\mu}{K} \simeq 2\alpha A(\alpha)\,\mu n,$$
$$\beta = -\Big\{\frac{3}{2}p^2 + \mu[(2p-1)A + 4B]\Big\}K^{-4} \simeq -\frac{3p^2 n}{2K},$$
$$\varepsilon = \frac{\mu C(\alpha)}{K^{1/2}} \simeq \alpha C(\alpha)\,\mu n K^{\frac{1}{2}}. \tag{24}$$

We note that the classical "small divisor", defined in terms of mean orbital elements, is related to the above-defined quantities as follows:

$$(p+1)n_2 - pn - g_0 = \omega + 2\beta J. \tag{25}$$

In practice, it is necessary to make two significant corrections to the above coefficients. (i) The mean motions are nominally given by $n_i = a_i^{-3/2}$. But these should be corrected for the effects of higher order gravitational

---

[3]The secular resonance Hamiltonian obtained in Eqn. 13 is similar in form to the first order mean motion resonance Hamiltonian of Eqn. 23. The major difference is that the coefficient of the nonlinear term, β, is not small in the case of mean motion resonances. The analysis of the scaled resonance Hamiltonian (obtained below) is directly applicable to the secular resonance as well.

harmonics of the planet, and also for the effects of the constant part of the disturbing potential of the satellite system. (ii) The expression for g_0 given above is the precession rate induced by the average secular perturbations of the perturbing satellite m_2 alone. Contributions from the higher order gravitational harmonics of the planet, as well as the average secular perturbations from other satellites should be added to this rate. These corrections are important when evaluating the "small divisor" (see Eqn. 36 below).

Because λ is a cyclic variable in this model, its conjugate momentum, K, is a constant of the motion. This provides a useful relationship between the resonance-induced variations of the semimajor axis and eccentricity:

$$\frac{\delta a}{a} \approx -p\delta e^2. \tag{26}$$

Therefore, from this relation, we can anticipate that the resonant perturbations in a are much smaller than those in e, a fact that justifies the approximation made in evaluating the coefficients A, B, C (see discussion following Eqn. 19).

The following scaling is useful for simplifying the analysis further. We define

$$
\begin{aligned}
J &= I \cdot \left|\frac{\varepsilon}{2\beta}\right|^{2/3}, & \omega &= -\nu \cdot 3\beta \left|\frac{\varepsilon}{2\beta}\right|^{2/3}, \\
\theta &= \begin{array}{ll} \text{sign}(\beta)\phi & \text{if} \quad \beta\varepsilon < 0, \\ \text{sign}(\beta)\phi + \pi & \text{if} \quad \beta\varepsilon > 0. \end{array}
\end{aligned}
\tag{27}
$$

The scaled resonance hamiltonian is given by

$$
\begin{aligned}
H &= -3\nu I + I^2 - 2\sqrt{2I}\cos\theta \\
&= -\frac{3}{2}\nu(x^2 + y^2) + \frac{1}{4}(x^2 + y^2)^2 - 2x,
\end{aligned}
\tag{28}
$$

where

$$(x, y) = \sqrt{2I}(\cos\theta, \sin\theta) \tag{29}$$

are the Poincaré variables. From the scaling relations in Eqn. 27 and the definitions of the coefficients in Eqn. 24, the eccentricity is (to lowest order) proportional to the distance from the origin in the (x, y) plane:

$$e \simeq \left|\frac{\alpha C(\alpha)}{3p^2}\mu\right|^{\frac{1}{3}}\sqrt{x^2 + y^2}. \tag{30}$$

The (scaled) single resonance Hamiltonian, Eqn. 28, has one free parameter, ν, and the topology of the phase space changes with the value of ν, as illustrated in Fig. 5. All phase space trajectories are periodic, but a separatrix, whose period is unbounded, exists for ν greater than a critical value, $\nu_{\text{crit}} = 1$. The separatrix divides the phase space into three zones: an external and an internal zone and a resonance zone. Most orbits in the resonance zone are librating orbits, i.e. the resonance angle executes finite amplitude oscillations, whereas most orbits in the external and internal zones are circulating orbits (i.e. θ increases or decreases without bound).
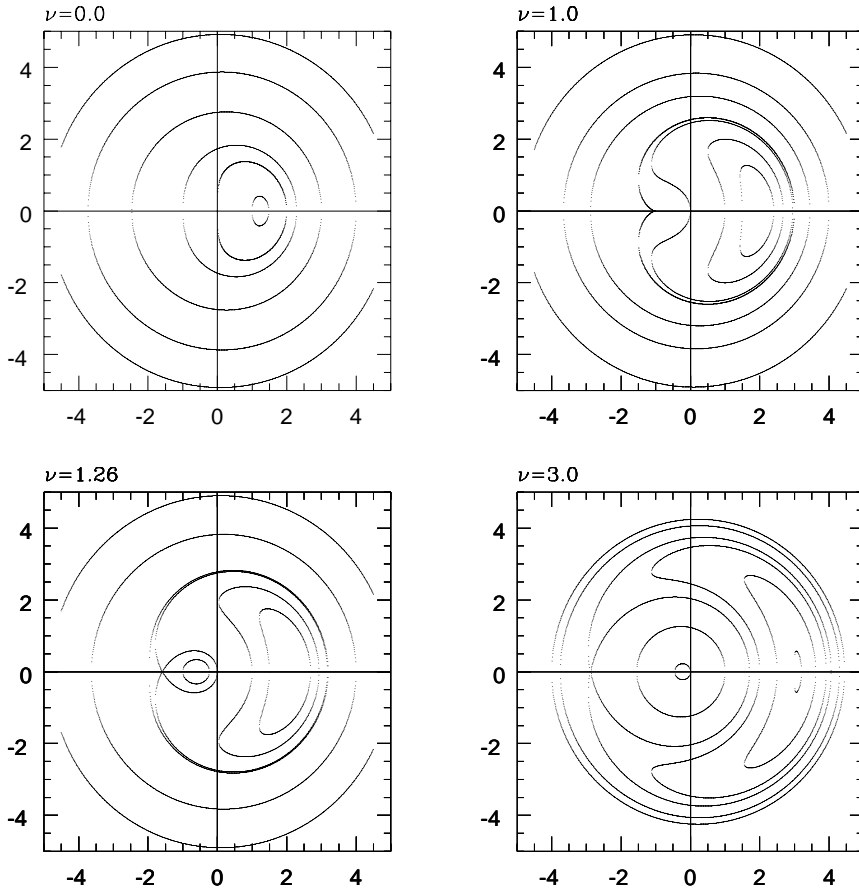
51

Figure 5.   Phase space topology of a first order resonance for four representative values of ν.

Many useful results on the phase space and dynamics of the single resonance Hamiltonian, including adiabatic evolution owing to a slow variation of the parameter ν, are given in (Henrard & Lemaitre, 1983; Lemaitre, 1984; Malhotra, 1988.) Below we mention a few interesting points, particularly concerning the behavior of particles starting at the origin in the (x, y) plane, i.e. initially circular orbits.

5.4.   Resonance width

For $|\nu| \gg 1$, the resonantly forced oscillations in (x, y) of particles on initially circular orbits are nearly sinusoidal, with frequency 3ν and amplitude $\sim \frac{2}{3}|\nu|^{-1}$. In the vicinity of $\nu \approx 0$, the oscillations are markedly non-sinusoidal, and have a maximum amplitude of $2^{\frac{5}{3}}$ at $\nu = 2^{\frac{1}{3}}$. There is a discontinuity at this value of ν: just above $\nu = 2^{\frac{1}{3}}$, the amplitude drops to half the maximum. Fig. 6 illustrates these points. (We note in passing that $\nu = 2^{\frac{1}{3}}$ represents a period-doubling transition point.)
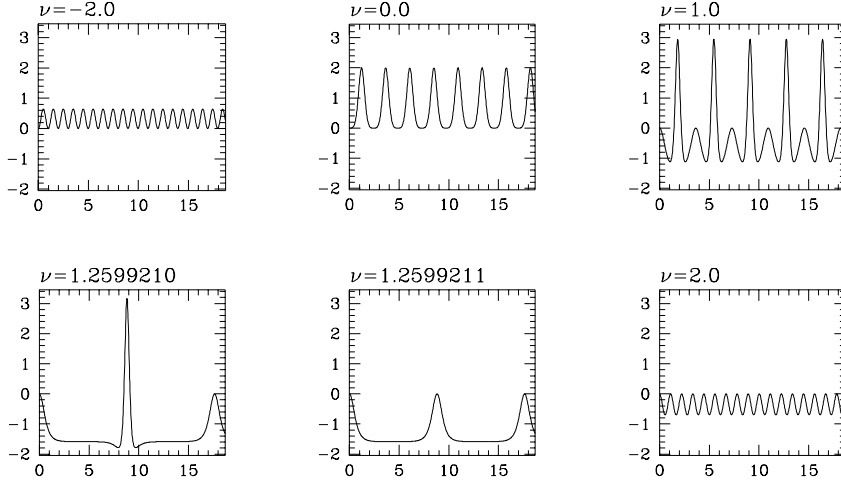
52

Figure 6. The time evolution of x for a particle initially at the origin, for various values of ν.

On the other side of the maximum, the half-maximum amplitude occurs at a value of $\nu \simeq -0.42$. Thus, we can define the resonance full-width-at-half-maximum amplitude *for initially circular orbits*:

$$\Delta\nu_{\mathrm{fwhm}} \approx 2. \tag{31}$$

Using the scaling relations (Eqns. 27), we can define the resonance width in terms of the mean motion of the inner satellite:

$$p\Delta n \approx \left|9p\alpha C(\alpha)\,\mu\right|^{\frac{2}{3}}n. \tag{32}$$

and the maximum eccentricity excitation of initially circular orbits:

$$e_{\mathrm{max}} \simeq 2\left|\frac{4\alpha C(\alpha)}{3p^2}\,\mu\right|^{\frac{1}{3}}. \tag{33}$$

For eccentric orbits (equivalently, large values of ν), the resonance width is defined by the extrema of I on the separatrix which encloses the center of libration (see Fig. 5). This is given by $\Delta I = (I_{\mathrm{max}} - I_{\mathrm{min}})_{\mathrm{separatrix}} \approx 4(3\nu)^{\frac{1}{4}}$, which can be translated into a width in mean motion:

$$\Delta n \simeq 4\left|3\alpha C(\alpha)\,\mu\bar{e}\right|^{\frac{1}{2}}n, \tag{34}$$

where $\bar{e}$ is the (forced) eccentricity at the center of libration. For future reference, we note that the frequency of small amplitude oscillations about the resonance center is given by

$$\omega_0 \simeq \left|3p^2\alpha C(\alpha)\,\mu\bar{e}\right|^{\frac{1}{2}}n. \tag{35}$$

53

5.5. Adiabatic evolution

The behavior of initially circular orbits to adiabatic changes of ν (due to external forces) is of particular interest in the evolution of orbits across mean motion resonances in the presence of small dissipative forces. Of course, in the presence of dissipation, the actual trajectories are not closed in the (x, y) phase plane, but the level curves of the single resonance Hamiltonian (Fig. 6) serve as guiding trajectories for such dissipative evolution. We can gain considerable insight into the evolution near resonance by using the well-known result that that the action is an adiabatic invariant of the motion in a Hamiltonian system. For the single resonance Hamiltonian, the action is simply the area enclosed by a phase space trajectory in the (x, y) plane. Thus we can state that for guiding trajectories which remain away from the separatrix, adiabatic changes in ν preserve the area enclosed by the guiding trajectory in the (x, y) phase plane, even as the guiding center moves. There are two possible guiding centers corresponding to the two centers of libration of θ (Fig. 6). Fig. 7 shows the location of these fixed points (all of which occur on the x-axis, i.e. at $\theta = 0$ or π) as a function of ν.

For a particle initially in a circular orbit, approaching the resonance from the left, i.e. ν increasing from initially large negative values, the initial guiding trajectory has zero enclosed area. This is the case when the initial "free eccentricity" is vanishingly small, and the particle's eccentricity is determined by the resonant forcing alone. Such an orbit adiabatically follows the positive branch in Fig. 7, so that as ν evolves to large positive values, the particle's eccentricity is adiabatically forced to large values as the guiding center moves away from the origin. The positive branch corresponds to the center of libration at $\theta = 0$ (where the small divisor $(p + 1)n_2 - pn - g_0$ has the same sign as the coefficient $-C(\alpha)$ of the resonant term); this guiding center is defined by

$$\bar{x} \simeq \sqrt{3\nu} \quad \text{for} \quad \nu \gg 1, \qquad \text{equiv.} \qquad \bar{e} \simeq \frac{-\alpha C(\alpha)\,\mu n}{(p + 1)n_2 - p\bar{n} - g_0}. \tag{36}$$

where $\bar{e}$ and $\bar{n}$ are the mean elements at the center of libration. The adiabatic rate of increase of the resonantly forced eccentricity along the positive branch is given by

$$\left\langle \frac{d\bar{e}^2}{dt} \right\rangle \simeq \frac{2}{3p} \left\langle \frac{\dot{n}_2}{n_2} - \frac{\dot{n}}{n} \right\rangle_{\text{ext}} + \left\langle \frac{de^2}{dt} \right\rangle_{\text{ext}} \tag{37}$$

where the subscript 'ext' refers to the contribution due to the external dissipative forces.

The guiding trajectory will be forced to cross the separatrix if the initial area enclosed by it exceeds an area equal to $2\pi I_{\text{crit}} = 6\pi$, i.e. the area enclosed by the separatrix when it first appears at $\nu_{\text{crit}} = 1$. I_{crit} translates into a critical value of the initial "free eccentricity",

$$e_{\text{crit}} = \sqrt{6} \left| \frac{\varepsilon}{2\beta} \right|^{\frac{1}{3}} K^{-\frac{1}{2}} = \sqrt{6} \left| \frac{\alpha C(\alpha)}{3p^2} \mu \right|^{\frac{1}{3}}. \tag{38}$$

Negotiating the separatrix is difficult business, for the adiabatic invariance of the action breaks down close to the separatrix where the period of the guiding trajectory becomes arbitrarily long. However, the crossing time is finite in practice, and separatrix crossing leads to a quasi-discontinuous "jump" in the action; subsequently, the new action is
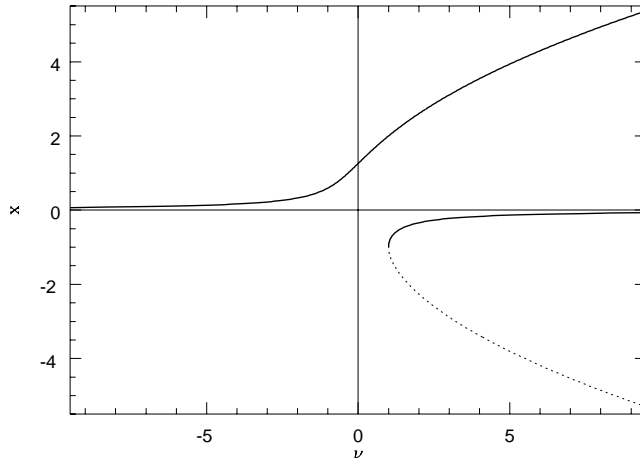
Figure 7.   The fixed points of the first order resonance Hamiltonian (Eqn. 28). For $\nu > 1$, the unstable fixed point on the separatrix is shown as a dotted line.

again an adiabatic invariant. One can define a probability of transition into the resonance libration zone by assuming a random phase of encounter of the guiding trajectory with the separatrix. A delicate analysis of this phenomenon was first carried out by independently by Neishtadt (1975), Yoder (1979) and Henrard (1982).

Finally, let us consider the evolution of a particle initially in a circular orbit, approaching the resonance from the right, i.e. ν decreasing from initially large positive values. In this case, the guiding trajectory adiabatically follows the negative branch in Fig. 7. However, the center of librations on the negative branch merges with the unstable fixed point on the separatrix at $\nu_{\text{crit}} = 1$, and the guiding trajectory is forced to negotiate the separatrix. There occurs a discontinuous change in the guiding trajectory which becomes briefly nearly coincident with the separatrix. Thereafter, as ν continues to decrease, the separatrix disappears, and the guiding trajectory becomes increasingly circular about the origin, with an area equal to $2\pi I_{\text{crit}} = 6\pi$, which is the area enclosed by the separatrix at $\nu_{\text{crit}} = 1$. Thus, in this case, passage through resonance leaves the particle with an excited "free eccentricity" equal to e_{crit} (Eqn. 38).

6.   Overlapping mean motion resonances

We have mentioned previously that the interaction between neighboring resonances is qualitatively the most significant when the widths of the resonances are comparable to their separation. In this section, we will discuss two distinct types of resonance overlap phenomena encountered in the Solar system. In the first, our discussion is in the context of the planar circular restricted three body problem where the splitting of a mean motion resonance does not occur but distinct mean motion resonances can overlap in the vicinity of the planet's orbit causing large scale chaos. The second case we discuss is the situation where the mean motion resonance splitting is significant but there is also significant coupling between neighboring sub-resonances.

55

6.1. Chaos in the circular planar restricted three body problem

In the circular planar restricted three body problem, there is no splitting of mean motion resonances, and in the first approximation, we can treat each mean motion resonance as a single isolated resonance. For near-circular test particle orbits, the single resonance model derived in Section 5.3 applies, and we can directly use those results. For $p \gg 1$, the resonance coefficient $C(\alpha)$ (Eqn. 20) evaluated at the resonance center, $\alpha = \alpha_{\mathrm{res}} = (1 + 1/p)^{-2/3}$, has the following simple approximation:

$$C(\alpha) \simeq \frac{p}{\pi}[2K_0(2/3) + K_1(2/3)] \simeq 0.80\,p, \tag{39}$$

where K_i are modified Bessel functions. With this approximation, the sum of the half-widths of neighboring mean motion resonances from Eqn. 31 is

$$\Delta_w n \approx 3.73\,p^{\frac{1}{3}}\mu^{\frac{2}{3}}\,n_{\mathrm{p}}. \tag{40}$$

The separation between adjacent $p : p+1$ and the $p+1 : p+2$ resonances is

$$\Delta_s n = \Big(\frac{p+1}{p+2} - \frac{p}{p+1}\Big)n_{\mathrm{p}} \approx p^{-2}n_{\mathrm{p}}. \tag{41}$$

An examination of Eqns. 40 and 41 shows that for a given μ there exists some value $p_{\min}$ such that the widths of first order resonances close to the planet with $p > p_{\min}$ will exceed their separation, and circular orbits in this region will exhibit the universal chaotic instability that arises from overlapping resonances.

More precisely, let us define the overlap ratio:

$$\gamma \equiv \frac{\Delta_w n}{\Delta_s n}. \tag{42}$$

The "two-thirds" rule states that the chaotic layers at the resonance separatrices merge — and most orbits in the vicinity of the resonances will be chaotic — when the overlap ratio γ is $\gtrsim 2/3$, i.e.

$$p^{-1} \lesssim 2.1\mu^{2/7}, \qquad \text{equiv.} \qquad \Big|\frac{a - a_{\mathrm{p}}}{a_{\mathrm{p}}}\Big| \lesssim 1.4\mu^{\frac{2}{7}}. \tag{43}$$

The above equation defines the extent of the chaotic region in the vicinity of a planet's orbit where heliocentric circular test particle orbits are unstable and become planet-crossing within a few synodic periods. Fig. 8 provides an illustration of the phenomenon of first order mean motion resonance overlap.

This result, often referred to as the "$\mu^{2/7}$ law", was first derived by Wisdom (1980) who used a slightly different definition of resonance width and obtained a slightly different numerical coefficient. The coefficient derived here is in close agreement with the numerical estimates of Duncan *et al.*, 1989.

The chaotic zone defined by the resonance overlap region does not preclude the existence of small regions of quasiperiodic orbits embedded within it. An obvious example
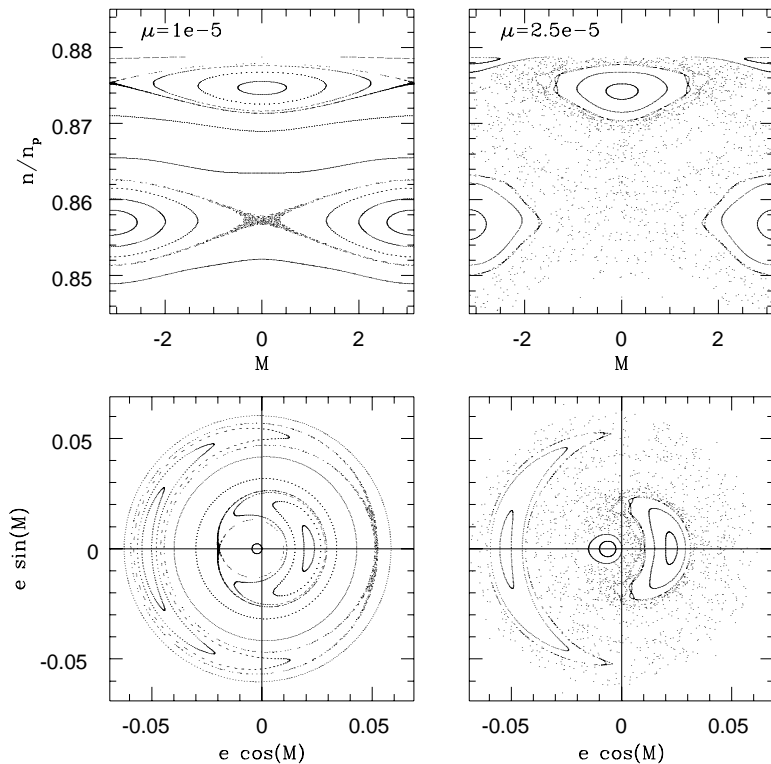
Figure 8. Surfaces-of-section for the circular planar three body problem illustrating the merging of the 7/6 and the 8/7 mean motion resonance separatrices as μ increases. The upper and lower panels represent different views of the same orbits, and are related by the Jacobi integral. These sections were obtained with a version of the mapping derived in Duncan *et al.*, 1989. (The mapping was corrected to make it area-preserving.)

is the stable libration zones at the classical Lagrange points where the mean motion of test particles is locked in 1:1 resonance with that of the planet. Small libration zones persist in the vicinity of other mean motion resonances as well, such as indicated in Fig. 8. Mean motion resonances outside the $\mu^{\frac{2}{7}}$ resonance overlap zone also have chaotic layers in the vicinity of their separatrices, with layer thickness diminishing with mean distance from the planet but a strong function of the mean eccentricity.

6.2. Interacting subresonances and secondary resonances

The simplest analytical model for interacting subresonances at a mean motion commensurability is obtained by treating a neighboring subresonance as a perturbation on the single resonance model. The form of the resonant terms in the perturbation potential (Eqn. 18) suggests the following form for the "perturbed resonance model":

$$H = \omega J + \beta J^2 + \varepsilon(2J)^{q/2}\cos q\phi + \varepsilon_1\sqrt{2J}\cos(\phi - \Omega t) \tag{44}$$
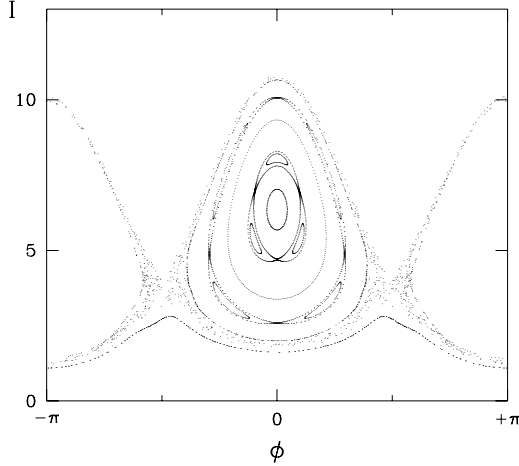
57

Figure 9. A surface-of-section for the perturbed resonance model (Eqn. 44, with $q = 2$) showing the apparition of secondary resonances due to the interaction of neighboring subresonances at a mean motion commensurability.

where we have generalized the single resonance Hamiltonian of Eqn. 23 to the qth order, and the last term describes the perturbation. In this model, which captures the essential elements of the dynamics of interacting subresonances, the primary subresonance (which we will refer to as simply the primary resonance) is described by the resonance angle, ϕ; it is perturbed by a neighboring subresonance ϕ'; the latter is approximated as $\phi' = \phi - \Omega t$, where the perturbation frequency Ω is the frequency splitting between the two subresonances; Ω is insensitive to J and can be assumed constant. We see then that two properties of the resonant perturbations conspire to cause a breakdown of the single resonance dynamics: the strength of the primary resonance increases with J as does the frequency of its small amplitude librations, and the strength of the perturbation also increases with J.

For the case where neighboring subresonances are of comparable strength (a circumstance often realized in satellite systems of the giant planets), the resonance overlap ratio can be defined as

$$\gamma = \frac{4\omega_0}{\Omega}, \tag{45}$$

where ω_0 is the small amplitude libration frequency of the primary resonance (see Eqn. 35). For $\gamma \ll 1$, i.e. Ω large compared to the libration frequency, the single resonance model is recovered by the averaging principle. Also, for $\Omega \longrightarrow 0$, the single resonance approximation is valid. As before, we can anticipate large scale chaos when $\gamma > 2/3$.

But for γ in the neighborhood of $2/3$, there is a very complex self-similar phase space structure with nested layers of secondary resonances embedded within the primary resonance. For the first level, consider the Fourier decomposition of the perturbation term when (J, ϕ) lies in the primary resonance libration zone:

$$\sqrt{2J} \cos(\phi - \Omega t) = \sum_{k=-\infty}^{k=+\infty} A_k \cos[(k\omega - \Omega)t + \delta]. \tag{46}$$

58

Here ω is the unperturbed libration frequency of ϕ; the coefficients A_k are exponentially small for large $|k|$. Within the primary resonance, the unperturbed libration frequency ω has a maximum value ω_0 at the center of the resonance zone and decreases to zero towards the separatrix. Therefore, for $\Omega \gg \omega$, the secondary resonance commensurability condition, $k\omega = \Omega$ is satisfied close to the separatrix for sufficiently large k. In fact, all secondary resonances with $|k|$ greater than some $k_{\min}$ will overlap and broaden the separatrix into a chaotic layer (see Fig. 9). The width of the chaotic separatrix is exponentially sensitive to the overlap ratio (Chirikov 1979):

$$\Delta H_{\mathrm{sx}} \sim \frac{\varepsilon_1 \sqrt{2J}}{\gamma^3} \exp(-\frac{2\pi}{\gamma}), \tag{47}$$

where H_{sx} is the energy of the unperturbed separatrix of the primary resonance.

When the splitting frequency, Ω, is a small-integer multiple of the small amplitude libration frequency ω_0, the fixed point at the center of the libration zone in the main resonance splits into a chain of secondary resonances[4]. This is illustrated in Fig. 9 which shows a surface-of-section of the perturbed resonance model for $3\omega_0 \approx \Omega$. The secondary resonances exhibit a self-similarity with the primary resonances, and the generic single resonance Hamiltonian (Eqn. 28) applies to these as well (Malhotra & Dermott, 1990; Malhotra, 1990; Engels & Henrard, 1994).

6.3. Adiabatic evolution

The appearance of secondary resonances at the center of a primary resonance leads to a new phenomenon in the evolution of bodies across mean motion resonances: an orbital mean motion resonance may be disrupted by means of capture into a secondary resonance. This mechanism is illustrated schematically in Fig. 10. The evolution proceeds as follows. Consider a particle with initially near-zero J approaching a mean motion commensurability along the positive branch, as discussed in section 5.5 above. It is first captured into a primary resonance, where the mean motion commensurability is maintained while the mean value of the canonical variable $\bar{J}$ is amplified. The perturbations from a neighboring subresonance imply that during this evolution, the particle will encounter secondary resonances which are born at the center of the primary resonance and migrate outward to the separatrix as $\bar{J}$ increases. For small-integer secondary resonances, capture into a secondary resonance becomes feasible. By the self-similar property, we can infer that the particle, upon capture into a secondary resonance, will adiabatically evolve along with the secondary resonance, and will be "dragged" out towards the separatrix of the primary resonance. However, the separatrix is really a chaotic layer (due to the accumulation and overlap of higher-integer secondary resonances). A particle which is forced into this chaotic layer will eventually escape from the primary resonance.

The appearance of secondary resonances near the center of the primary resonance zone requires an extraordinarily delicate tuning of parameters to ensure small-integer

---

[4]One could anticipate the dynamics of this system by noting that for $q = 1$ and for J not too small, Eqn. 44 is similar to the well-known parametrically perturbed pendulum which describes the resonant amplification of a swing in a playground.
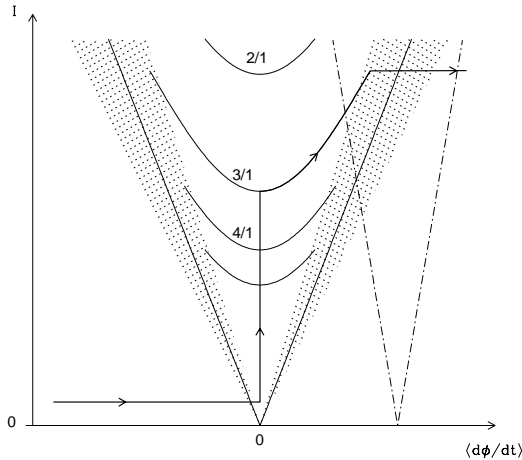
Figure 10.   A schematic illustration of the adiabatic evolution of a particle which is first captured in a mean motion subresonance, then captured in a secondary resonance and eventually ejected from the commensurability. The chaotic separatrix of the primary resonance is indicated by the shaded zone; the perturbing subresonance is shown by the dot-dash lines; the locations of several secondary resonances within the primary resonance are also indicated to scale.

commensurabilities between the splitting frequencies and the libration frequencies of the primary (sub)resonances. Amazingly enough, there is evidence that such a tuning of parameters was realized in the Uranian satellite system. We have remarked previously that at present there are no resonance librations amongst these satellites, although there are several near-resonances (cf. Fig. 4). Analysis of the long term orbital history has shown that owing to slow tidal evolution of the satellite orbits, several of these near-commensurabilities could have been exact resonances in the past which were disrupted by the action of secondary resonances in the manner described above. In particular, passage through the 1/3 mean motion resonance between Miranda and Umbriel and its disruption by means of a 1/3 secondary resonance accounts very well for Miranda's anomalously high orbital inclination, and temporary residence in eccentricity-type mean motion resonances may also help explain the complex thermal history of these satellites inferred from their surface appearance (Tittemore & Wisdom, 1990; Malhotra & Dermott, 1990).

7. Epilogue

Orbital resonance phenomena in the Solar system appear on a diverse range of timescales. Orbital resonances are the source of both stability and chaos, depending sensitively upon parameters and initial conditions. This fundamental conclusion and an understanding of its implications is leading a resurgence in the field of celestial mechanics, with import for planetary science in general. In this lecture, we have provided an overview of orbital resonance phenomena, with simple conceptual models that guide our understanding. The progress in recent years has already led to radically new views on the origin of orbital configurations and the distribution of small bodies in the Solar system. Many fundamental questions remain, particularly those pertaining to the origin and evolution of the orbital characteristics of generic planetary systems. We anticipate significant progress in these matters in the near future.

References

Brouwer, D. and G.M. Clemence (1961). *Methods of Celestial Mechanics*, Academic Press, New York.

Black, G.J.; Nicholson, P.D.; Thomas, P.C. (1995). Hyperion: Rotational dynamics, *Icarus* **117**:149-161.

Chirikov, B.V. (1979). A universal instability of many-dimensional oscillator systems, *Physics Reports* **52**(5):265-379.

Duncan, M., Quinn, T., Tremaine, S. (1989). The long term evolution of orbits in the solar system: a mapping approach, *Icarus* **82**:402-418.

Ellis, K.M. and Murray, C.D. (1998). The disturbing function in solar system dynamics, *Icarus* (submitted for publication).

Engels, J.R. and Henrard, J. (1994). Probability of capture for the second fundamental model of resonance, *Cel. Mech.& Dyn. Astron.* **58**:215-236.

Farinella, P., Froeschle, Ch., Froeschle, C., Gonczi, R., Hahn, G., Morbidelli, A. and Valsecchi, G.B. (1994). Asteroids falling onto the Sun, *Nature* **371**:315–317.

Goldreich, P. (1965). An explanation of the frequent occurrence of commensurable mean motions in the Solar system, *MNRAS* **130**(3):159-181.

Goldreich, P. and Tremaine, S. (1982). The dynamics of planetary rings, *Ann. Rev. Astron. Astrophys.* **20**:249-283.

Hamilton, D.P. (1994). A comparison of Lorentz, planetary gravitational, and satellite gravitational resonances, *Icarus* **109**:221-240.

Henrard (1982). Capture into resonance: an extension of the use of the adiabatic invariants, *Cel. Mech.* **27**:3-22.

Henrard, J. and A. Lemaitre (1983). A second fundamental model for resonance, *Cel. Mech.* **30**:197-218.

Holman, M., Touma, J. and Tremaine, S. (1997). Chaotic variations in the eccentricity of the planet orbiting 16 Cyg B, *Nature* **386**:254-256.

Holman, M.J. and Wisdom, J. (1993). Dynamical stability in the outer Solar system and the delivery of short period comets, *Astron. J.* **105**:1987–1999

Jewitt, D., J. Luu and J. Chen (1996). The Mauna Kea–Cerro Tololo (MKCT) Kuiper Belt and Centaur Survey, *Astron. J.* **112**:1225-1238.

Klavetter, J.J. (1989). Rotation of Hyperion. I. Observations, *Astron. J.* **97**:570-579.

Kozai, Y. (1962). *Astron. J.* **67**:591-598.

Laskar, J. (1994). Large scale chaos in the Solar system, *Astron. & Astrophys.* **287**:L9-L12.

Laskar, J. (1996). Large scale chaos and marginal stability in the Solar system, *Cel. Mech.& Dyn. Astron.* **64**:115-162.

Lemaitre, A. (1983). High order resonance in the restricted three-body problem, *Cel. Mech.* **32**:109-126.

Levison, H.F. and Duncan, M.J. (1993). The gravitational sculpting of the Kuiper Belt, *Astrophys. J.* **406**:L35–L38

Malhotra, R. (1988). PhD thesis, Cornell University.

Malhotra, R. (1990). Capture probabilities for secondary resonances, *Icarus* **87**:249-264.

Malhotra, R. (1993). The origin of Pluto's peculiar orbit, *Nature* **365**:819-821.

Malhotra, R. (1995). The origin of Pluto's orbit: implications for the Solar system beyond Neptune, *Astron. J.* **110**:420-429.

Malhotra, R. (1998). Pluto's inclination excitation by resonance sweeping, *LPSC-XXIX*, abstract no. 1476.

Malhotra, R. and S.F. Dermott (1990). The role of secondary resonances in the orbital history of Miranda, *Icarus* **85**:444-480.

Malhotra, R. and J.G. Williams (1997). Pluto's heliocentric orbit, in *Pluto and Charon*, eds. S.A. Stern and D. Tholen, Univ. of Arizona Press, Tucson, AZ.

Morbidelli, A. (1993). Asteroid secular resonant proper elements, *Icarus* **105**:48-66.

Morbidelli, A. (1997). Chaotic diffusion and the origin of comets from the 2/3 resonance in the Kuiper Belt, *Icarus* **127**:1-12.

Morbidelli, A., Gonczi, R., Froeschle, Ch. and Farinella, P. (1994). Delivery of meteorites through the ν_6 secular resonance, *Astron. & Astrophys.* **282**:955-979

Morbidelli, A. and Moons, M. (1993). Secular resonances in mean motion commensurabilities, *Icarus* **102**:1-17.

Neishtadt, A.I. (1975). Passage through a separatrix in a resonance problem with a slowly-varying parameter, Journal of Applied Mathematics and Mechanics, **39**(4):594-605 (translation).

Peale, S.J. (1986). Orbital resonance, unusual configurations, and exotic rotation states among planetary satellites, in *Satellites*, eds. J. Burns and M. Matthews, University of Arizona Press, Tucson.

Showman, A. and R. Malhotra (1997). Tidal evolution into the Laplace resonance and the resurfacing of Ganymede. *Icarus* **127**:93-111.

Tittemore, W.C. and J.W. Wisdom (1990). Tidal evolution of the Uranian satellites: III. Evolution through the Miranda–Umbriel 3:1, Miranda–Ariel 5:3, and Ariel–Umbriel 2:1 mean–motion commensurabilities, **Icarus 85**:394-443.

Wisdom, J. 1980. The resonance overlap criterion and the onset of stochastic behavior in the restricted three body problem, *Astron. J.* **85**:1122-1133.

Wisdom, J., Peale, S.J., Mignard, F. (1984). The chaotic rotation of Hyperion, **Icarus 58**:137-152.

Yoder, C.F. (1979). Diagrammatic theory of transition of pendulum-like systems, *Cel. Mech.* **19**:3-29.